Chapter

G-Jitter, Vibrations, Diffusion: The IVIDIL Experiment

Valentina Shevtsova, Denis Melnikov, Yuri Gaponenko and Aliaksandr Mialdun

Abstract

Experiments aboard the International Space Station (ISS) provide a large but still limited amount of data. A complete set of data is usually returned to Earth on a flash disk a few months later, by which time the experimental facility has already been put into storage or trashed. Thus, scientists have no possibility to repeat the experiment, even if some ambiguities are later found. Therefore, onboard experiments require careful preparation on the ground with multiple tests in the laboratory and in parabolic flights, if possible. Furthermore, during postflight analysis, it is important to clarify all unknown sources of errors. One of the most obvious sources of perturbations on the ISS is g-jitter. Here, we present the preparation and implementation of the Influence of Vibrations on Diffusion in Liquids (IVIDIL) experiment on the ISS, which studied the effect of random g-jitter and given vibrations on diffusion-controlled experiments in liquid mixtures. Since diffusion in liquids is a slow process, only vibrational effects were examined in parabolic flights. A methodology for the analysis of diffusion and thermodiffusion processes was developed in the laboratory.

Keywords: ISS, IVIDIL, parabolic flight, vibration, Soret effect

1. Introduction

The authors of this chapter work at the Microgravity Research Centre of the Free University of Brussels (Université libre de Bruxelles, ULB) and form the core of the research group "Nonlinear phenomena in fluids." Primarily, we are interested in the behavior of fluids in a low-gravity environment and application of the results in Earth-based technologies. We carry out research in the field of physics of fluids, applied mathematics, process/chemical engineering and transport phenomena. More precisely, we are particularly interested in the following topics: vibrational phenomena in fluids, interfacial heat and mass transfer (with application to material science), controlling the flow in thermocapillary liquid bridges embedded in a gas stream, diffusion and Soret effect in free liquids and porous media and transport of impurities in the CO_2 storage. Recently, we have started a new research project related to an environmental issue, such as microplastic uptake by viscoelastic interfaces. Many of these topics trace their roots from the Influence of Vibrations on Diffusion in Liquids (IVIDIL) experiment, detailed below.

By combining theoretical, numerical (commercial codes, "home-made" codes) and experimental tools (essentially implementing methods of optical diagnostics: interferometry, shading, spectrometry), we obtain original results and publish them in high-stand journals. Our other strong points are the development of a fruitful cooperation with European and overseas research groups and the attraction of master and PhD students from all over the world.

2. G-jitter

Access to the microgravity environment provides the opportunity to perform fluid and materials science experiments designed to take advantage of near weightlessness. The term "near" underlines the unavoidable presence of uncontrolled accelerations due to aerodynamic drag, trembling of space vehicles, onboard machinery and crew activity. The fluctuating contribution of g(t) comprises a broad frequency spectrum. These random and periodic gravity fluctuations are referred to as gravity jitters (or g-jitter). The dedicated experimental studies of the effect of g-jitter on fluid systems in weightlessness were rather limited. Until recently, there was an open question: does g-jitter cause a sizeable mean flow, and, if so, does this mean flow promote striations and other defects in materials processing in microgravity? Thus, one of the objectives of one of the first experiments on the International Space Station (ISS) was to present experimental evidence of the role of the microgravity environment and, in particular, g-jitter. For this purpose, the IVIDIL project was proposed to the European Space Agency (ESA) in 2000 by an international team including the Microgravity Research Centre of ULB (Brussels, Belgium), the Institute of Continuous Media Mechanics UB RAS (Perm, Russia) and Ryerson University (Toronto, Canada) and coordinated by the Brussels team. The multiuser facility Selectable Optical Diagnostic Instrument (SODI) was designed and developed by the Belgian company QinetiQ Space (then Verhaert Space). The IVIDIL was the first experiment conducted inside the SODI.

The real need for such an extra experiment may be questioned because one option would be to use scaling analysis. Many analytical studies are restricted by the assumption of linearity, quasi-steadiness or very high/low frequencies. There is always a possibility that some of the aspects of a real experiment are not considered in theoretical hypotheses. Moreover, the failure of some microgravity experiments has been attributed to the effect of g-jitter.

3. Definition of the IVIDIL experiment

When the construction of the ISS was coming to an end, the goal of one of the first onboard experiments was to provide experimental evidence of the influence of the microgravity environment and, in particular, g-jitter, on diffusion-controlled experiments that refer to material science. This experiment was conducted in the SODI belonging to ESA.

The primary idea of the IVIDIL experiment was to measure diffusion coefficients in two binary mixtures in g-jitter environment and under different vibrational frequencies and amplitudes. For this reason, one should create controlled and reproducible concentration non-uniformity in the liquid. If it were generated on Earth, it would diffuse during the waiting time on the launch site that can last several months. It was decided to use the Soret effect for creating a concentration profile in the experimental cell.

The Soret effect (also known as thermodiffusion or thermal diffusion) is a molecular transport of substance associated with a thermal gradient. In response to this gradient, concentration gradients appear in an originally uniform mixture. It extended the objectives of the experiment to the measurements of the Soret coefficient as it has industrially and scientifically driven interests. During each experimental run, a temperature difference is established across the cell, to achieve a separation of components as induced by the Soret effect during 12 h. Then, the temperature difference is switched off, the cell is brought rapidly to isothermal conditions, and the components diffuse back to a homogeneous distribution. While the process takes place, the sample is shaken perpendicularly to the temperature and/or concentration gradient, with frequencies up to 2.8 Hz and amplitudes up to 68 mm.

The application of vibrations to a fluid system with density gradient can cause relative flows inside the fluid. If this gradient results from thermal or compositional variations, such flows are known as thermovibrational or solutovibrational convection, respectively. High-frequency and small-amplitude vibrations are of special interest, as they may create mean flows, an analogue of streaming flows in acoustic phenomena, which contribute to the transport of heat and mass in a time-average sense. Thus, the appearance and progress of vibrational convection in low gravity was another additional target. The test fluids were two different concentrations of water-isopropanol (IPA) with positive and negative Soret effect. The measured values in convection-free environment should be used as standards for ground experiments.

For one of the first experiments on the ISS, it may not sound very exciting, but it is very important for material sciences and may advance many everyday technological processes.

To summarize, the objectives of the IVIDIL experiment were the following:

- To present experimental assessment of the role of g-jitter
- To perform precise measurements of diffusion and thermodiffusion coefficients for two binary mixtures in g-jitter environment
- To disclose the influence of controlled vibrations on the measured values of diffusion and thermodiffusion coefficients
- To investigate vibration-induced convection and, particularly, heat and mass transfer under vibrations

In the frame of preparatory activities, the science team performed laboratory experiments [1–4], parabolic flights [5–8] and numerical calculations [9, 10].

4. Vibrational convection

Vibrational convection provides a mechanism of heat and mass transfer due to the existence of mean flows. This refers to small-amplitude and high-frequency vibrations, i.e. when the period is much smaller than the reference hydrodynamic times. In this case, the flow field can be decomposed into the “quick” part, which oscillates with the frequency of vibration, and the “slow” time-averaged part (mean flow), which describes the nonlinear response of the fluid to a periodic excitation [11].

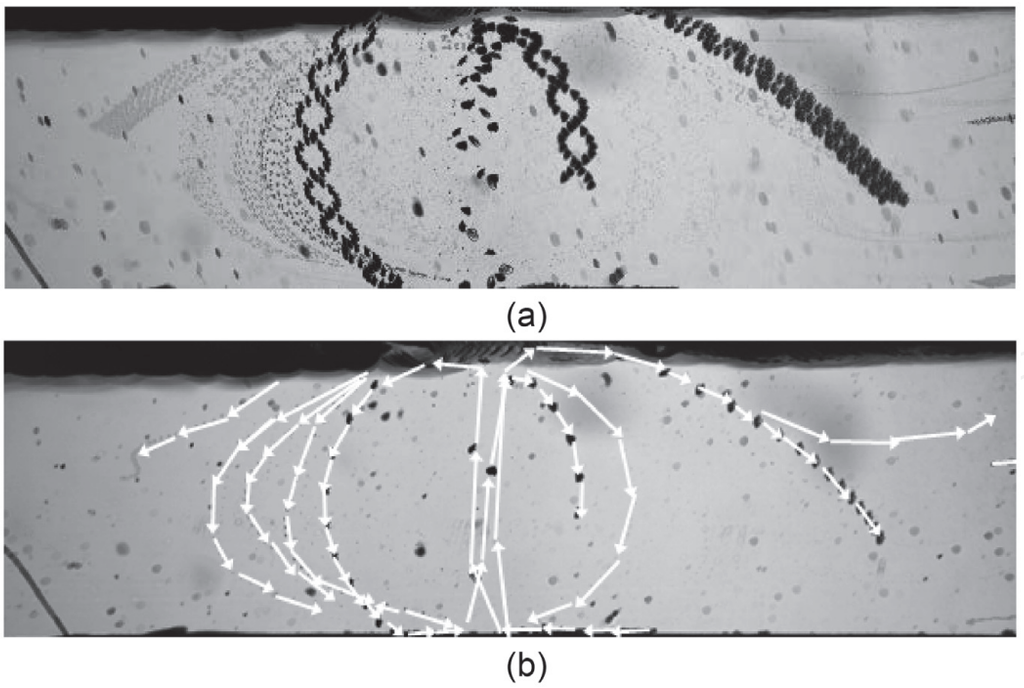

Figure 1.
(a) Image made with 500 superimposed images, keeping minimum pixel intensity for each pixel. The motion of particles illustrates the sum of "quick" and fast part of the flow [12]. (b) Mean flow tracing by selecting images at the same phase of the vibration period [12].

These two types of flow are illustrated by our experiments [12] in **Figure 1**. A few small particles of polytetrafluoroethylene (PTFE) with a characteristic diameter of particles between 20 and 80 μm were present in the cell. The rectangular cavity filled with water-isopropanol mixture was shaken in the horizontal direction with frequency f = 22 Hz and amplitude A = 3.5 mm. Small-amplitude oscillations, as well as average displacement of the particles, can be observed in **Figure 1a**. A fast oscillating contribution seen in the horizontal direction, which has the same frequency as the imposed external vibration, is superimposed on the mean flow with a slow characteristic time scale [6, 11]. The evolution of the mean flow without high-frequency contribution could be observed while selecting images at the same phase of the vibration period. The ensemble of particles in **Figure 1b** represents directly the mean flow without fast oscillations. The arrows in **Figure 1b** highlight the features of the mean flow, clearly demonstrating a flow pattern with two vortices near the cell center.

The effect of the mean flow is most pronounced in the absence of other external forces (in particular, static gravity which has a strong damping effect). In weightlessness, it is an additional way of transporting heat and matter similar to thermo- and solutocapillary convection. Mean flows show some similarity with gravity-induced convection and might serve as a way to control and operate fluids in space [13]. Vibrations can suppress or intensify gravitational convection depending on the mutual orientation of the vibration axis and thermal (compositional) gradient [14, 15].

There have been extensive *theoretical* studies of thermovibrational convection in weightlessness and ground conditions. The fundamental treatise [11] comprises a systematic study of convective flows induced by high- and finite-frequency vibrations in closed and infinite cavities. Thermovibrational convection in square, rectangular and cubic cavities was widely investigated providing a variety of mean flow structures and bifurcation scenarios [16–18]. The influence of vibration on double-diffusive convection with the Soret effect was also analyzed in [19–21].

Experimental studies of vibrational phenomena in weightlessness are rather limited. A series of experiments was carried out onboard the MIR station with the ALICE-2 instrument [22, 23] and DACON [24]. The influence of vibrations on the propagation of a temperature wave from a heat source in a near-critical fluid was investigated. Thermovibrational flows were registered by observing the optical inhomogeneity caused by the distortion of the temperature field. It was not possible to reconstruct this field quantitatively.

5. Preparation of the experiment IVIDIL in parabolic flights

Even though our colleague from MRC had already conducted many experiments in low-gravity environment, for our group, the IVIDIL was the first experiment in weightlessness. We felt an enormous responsibility and proposed to the ESA to conduct the experiment in parabolic flights. Parabolic flights provide repeated periods of approximately 20 seconds of reduced gravity g ≈ 0.01 g0 preceded and followed by 20 seconds of hypergravity (up to 1.8 g0), where g0 = −9.81 m/s^2.

Surely, during 20 s one cannot observe the diffusion or Soret process, and the aim of the parabolic flight experiment is to investigate the development of thermovibrational flows in low gravity and verify the existing theoretical studies. During our first parabolic flight, the TEVICON (Thermovibrational Convection [25]) experiments took place in 2007. A large contribution to the success of the experiment was made by Dr. I. Ryzhkov, who worked in our group at that time.

5.1 Theory and numerics

In addition to technical problems and rack design, observation of thermovibrational convection formed in 20 s required serious preparation. The primary task is to find the configurations, where the intensity of thermovibrational convection is significantly larger than that of thermal convection caused by the residual gravity. On the first stage of preparation, we used theoretical estimations and conducted numerical simulation of full Navier-Stokes equations in the closed cubic geometry [8, 9]. Dimensionless variables were introduced by taking the scales of length L, time L^2/ν, velocity ν/L, pressure $\rho_0\nu^2/L^2$ and temperature $\Delta T = T_{hot} - T_{cold}$. The dimensionless equations are written in the form

$$\begin{aligned} &\boldsymbol{u}_t + (\boldsymbol{u}\cdot\nabla)\boldsymbol{u} = -\nabla p + \nabla^2\boldsymbol{u} - (\boldsymbol{Gr} + Gr_v\cos(\Omega t)\boldsymbol{n})T, \\ &T_t + (\boldsymbol{u}\cdot\nabla)T = Pr^{-1}\nabla^2 T, \\ &\nabla\cdot\boldsymbol{u} = 0. \end{aligned} \tag{1}$$

Here, the dimensionless parameters are the Prandtl number, Pr; the Grashof number, Gr; the vibrational Grashof number, Gr_v; and the dimensionless frequency, Ω:

$$Pr = \frac{\nu}{\chi}, \quad \boldsymbol{Gr} = \frac{\boldsymbol{g}\beta_T\Delta T L^3}{\nu^2}, \quad Gr_v = \frac{A\omega^2\beta_T\Delta T L^3}{\nu^2}, \quad \Omega = \frac{\omega L^2}{\nu}, \tag{2}$$

where A is the amplitude of vibration, $\omega = 2\pi f$ is the angular frequency, $\boldsymbol{g}$ is the gravitational acceleration, β_T is the thermal expansion, v is the kinematic viscosity, χ is the thermal diffusivity, L is the characteristic size and ΔT is the applied temperature difference.

When a fluid is subjected to high-frequency vibration and density inhomogeneity is caused by the thermal gradient, the vibrational and gravitational convective mechanisms are characterized by alternative dimensionless parameters, such as the Rayleigh number, *Ra,* and the Gershuni number, Gs, its vibrational analogue:

$$Ra = \frac{g\beta_T \Delta T L^3}{\nu\chi}, \quad Gs = \frac{(A\omega\beta_T \Delta T L)^2}{2\nu\chi}. \tag{3}$$

The ratio Gs/Ra describes the relative importance of thermovibrational and gravitational convective mechanisms. The goal of the numerical study was to understand what kind of mean flow regimes can be observed during the short experimental time of 20 s and assess the influence of residual gravity on the transient process. It should be emphasized that we were interested in mean flows, which can induce heat transfer in a system subjected to external vibration.

It was well known from the previous theoretical studies [11] that in a rectangular cavity under weightlessness, a nonzero mean flow exists at any value of the Gershuni number, *Gs,* when the direction of vibration is perpendicular to the temperature gradient (this configuration was considered in our study). For small values of the Gershuni number, the stationary mean flow is weak and has a four-vortex symmetrical structure (see **Figure 2**, left). When the Gershuni number exceeds some critical value *Gscr*, a flow pattern bifurcates to the pattern with different symmetry: one large diagonal vortex and two small vortices in the corners (see **Figure 2**, right).

The presence of the residual gravity may strongly affect the flow pattern. The numerical simulations have shown that the residual gravity in the Z-direction can destabilize (stabilize) the flow when the gravity vector and the temperature gradient have the same (opposite) directions. Here, the temperature gradient is always codirected with the Z-axis. The *lateral* residual gravity (in the X-direction) is always destabilizing [6]. It holds even if the ratio of the numbers of Gershuni and Rayleigh, which describes the relative importance of vibrational and natural convection due to residual gravity, is very large. For example, the patterns in **Figure 2a** and **b** correspond to $Gs/Rax \sim 2.9 \cdot 10^5$. The sign of lateral residual gravity controls the inclination of the diagonal vortex and the direction of rotation in the steady state as seen from panels (a) and (b).

Next, we examined six different liquid candidates such as water, ethanol, methanol, isopropanol, pentane and transformer oil. The target was to identify the liquid which would provide the largest Gershuni number for the given frequency, amplitude and ΔT. From the definition of the Gershuni number (see Eq. (3)), it follows that this liquid should have large thermal expansion βT but small kinematic viscosity and thermal diffusivity. After detailed consideration, isopropanol has been selected as a working liquid.

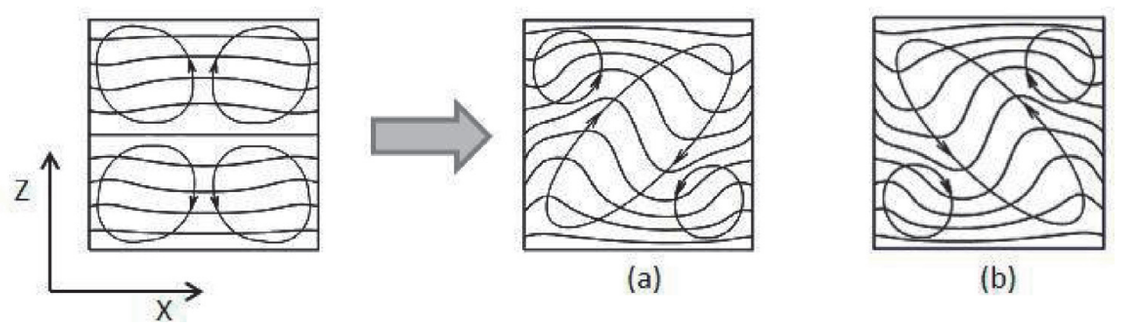

Figure 2.
(Left) Typical flow pattern of vibrational convection predicted theoretically for zero-gravity environment at low Gershuni number. (Right) The flow pattern (a) in presence of lateral gravity; (b) under the action of residual gravity in z-direction.

5.2 Experiment design

To observe thermovibrational convection in microgravity, we have designed a dedicated experimental set-up placed in special rack to be used during parabolic flights (see **Figure 3**, left). Here we provide the basic principles, and the more detailed description can be found elsewhere [5, 6]. The thermovibrational flows were monitored by measuring the temperature field inside the cell by optical digital interferometry. The set-up performance is based on the concept of Mach-Zehnder interferometer shown in **Figure 4**. The light beam of He-Ne laser is expanded by the spatial filter and then splits into two collimated beams of equal intensity by the beam splitter.

We knew about the cell design in the forthcoming IVIDIL experiment, and for the parabolic flight tests, similar (but scaled) cells from Hellma Company were ordered. The cell is made of Suprasil quartz. The internal part, which has a cubic shape with walls of size L = 5 mm, was filled with isopropanol. The external walls of

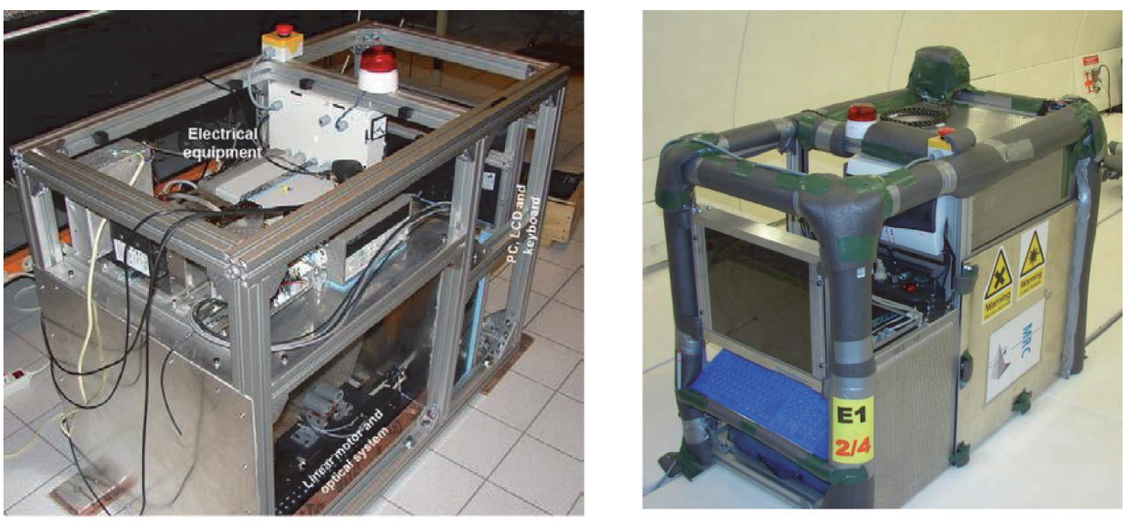

Figure 3.
Rack designed for the TEVICON-1 parabolic flight experiment in 2007.

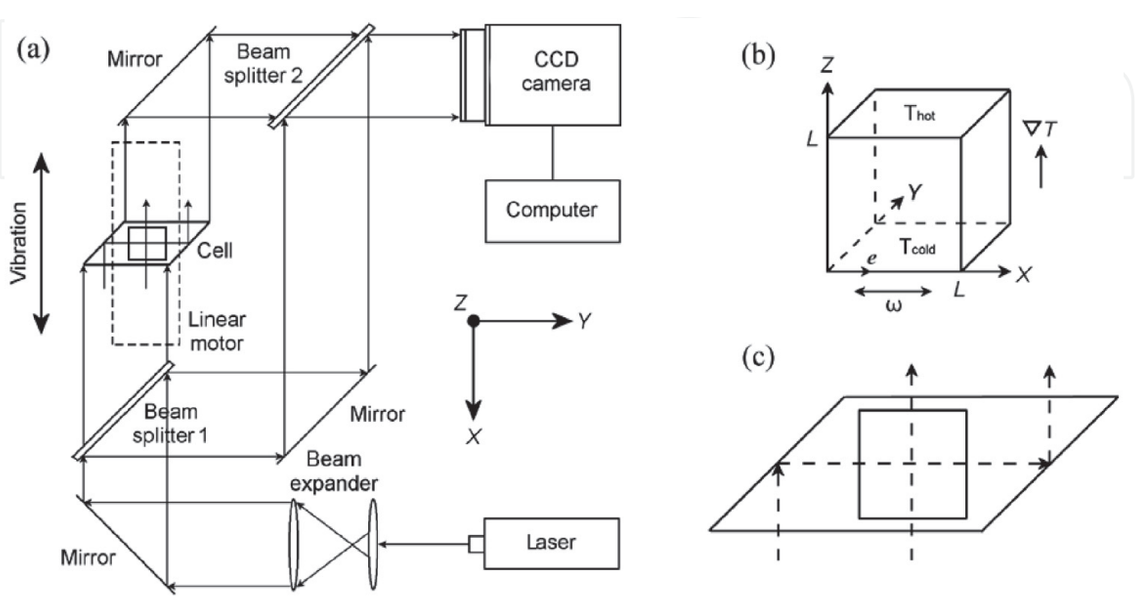

Figure 4.
(a) The scheme of experimental set-up, (b) the cubic cell filled with liquid and coordinate system and (c) the top view of the experimental cell.

the cell are shaped in the form of two transparent prisms (**Figure 4c**) to allow scanning of the front and side views (planes *YZ* and *XZ*, respectively). The beam paths through the cell are shown by the arrows. Due to the smart design of the cell, the objective beam transverses the entire cell in two perpendicular directions.

The top and bottom walls of the cell were kept at constant temperatures *Thot* and *Tcold*, respectively, by Peltier modules. In the experiments, the mean temperature was fixed at 40°C, while the applied temperature difference $\Delta T = Thot - Tcold$ was either 15 K or 20 K. The experimental cell was attached to the linear motor, which performs translational harmonic oscillations in the *X*-direction (perpendicular to the temperature gradient). In the coordinate system associated with the cell, the acceleration applied to the system is the sum of gravitational and vibrational accelerations:

$$\boldsymbol{g}(t) + A\omega^2 \cos(\omega t)\, \boldsymbol{e}, \tag{4}$$

where $\boldsymbol{g}(t) = (gx, gy, gz)$ is the time-dependent gravity vector and $\boldsymbol{e} = (1, 0, 0)$ is the unit vector along the axis of vibrations.

Repetition of the experiments with different vibration parameters and temperature gradients allows to recognize in what extent the thermovibrational convection is sensitive to microgravity and to define some regions of parameters with strong convective flows [6].

5.3 Two busy weeks during the parabolic flight campaign

After long and difficult months of trial and errors in the laboratory, all parts were assembled in a rack and passed numerous tests. Along with real experimental tests, there were a lot of technical reports required by the ESA contractor. Finally, the rack shown in **Figure 3** (left) was placed in a small truck and transported to Bordeaux-Mérignac, along with part of the team.

At our arrival at the Bordeaux-Mérignac airport, we realized that the problems were far from over. The first problem we faced was the thermal controller that was not working. After conducting multiple attempts and tests, we were not able to activate it. The time remaining before flights was rather short. We ordered a new controller on the Internet with an overnight delivery. The next morning, after installing the newly arrived controller, we were ready to cry, as it also did not work. We could not determine the reason. We knew that in our laboratory in Brussels there was another thermal controller, which had been used for several tests, and it worked. We asked Prof. J.C. Legros to bring it by car from Brussels to Bordeaux in the quickest possible way. After installing and testing it, the team cheered with relief: it worked!

Even though the instrument was working, we still needed to go through several control tests, e.g. leak tightness of all the volumes with liquid, safety checks, etc., before being allowed to move the instrument into the plane. One may see our happy faces in **Figure 5** (left), when the rack was allowed into the plane. After a difficult week of problem-solving, we thought it was finally time to fly!

But the obstacles were not over yet. While inside the specialized "Zero-G" aircraft, our rack again needed to undergo a series of control checks by a large team of experts from the *Centre d'Essais en Vol* (CEV, French Test Flight Centre) (see right picture in **Figure 5**). All these controls ended on the eve of the flight experiment day.

The first day of parabolic flights is very exciting. On the one hand, there is the responsibility for the success of the experiment and, on the other hand, a concern

Figure 5.
Rack is transferred to the plane.

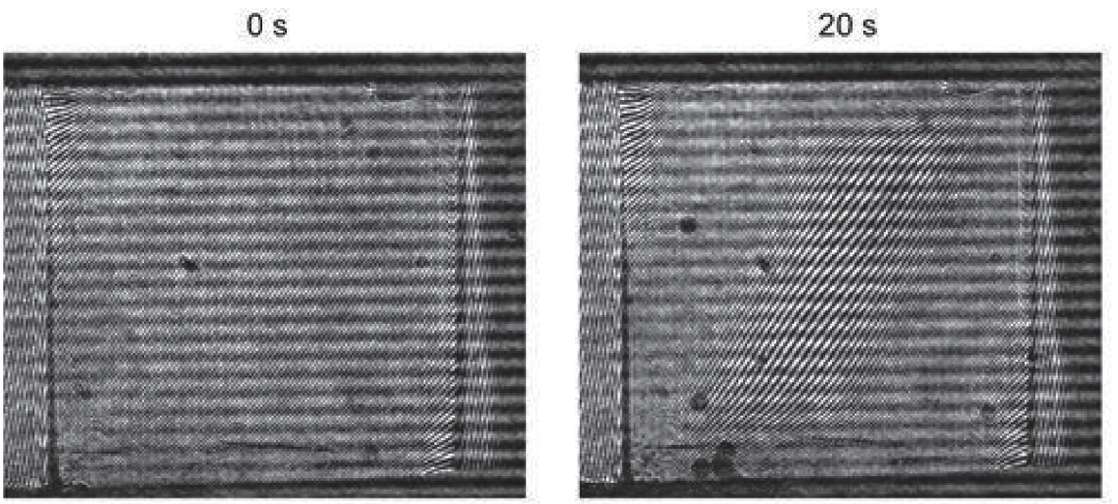

Figure 6.
Interference patterns of the side view of the cell at different times, f = 4 Hz, A = 45 mm, ΔT = 20 K.

for one's own well-being. After all the effort and the stress of preparation, we were delighted to see that everything went well and without considerable problems. We managed to get excellent scientific results, subsequently published in high-stand journals!

5.4 Scientific and strategic results out of TEVICON experiment

Figure 6 presents the acquired interference patterns of the cell at 0 and 20 s from the start of vibration. During parabolic flight experiments, we watched only black-and-white images and visually drew a conclusion about the power of convection. In the first frame (0 s), the pattern is formed by the interchange of the thin black and white lines (fringes).

These lines are inclined and almost parallel; in addition, they have the same thickness except for the regions near the lateral walls, where temperature slightly deviates from purely conductive state. In the second frame (20 s), we see that the thickness of fringes increases in the diagonal from the bottom left to the top right corner. Around this diagonal, the thickness decreases. In addition, the deformation of fringes becomes larger. All these changes result from the deformation of the temperature field by thermovibrational convection.

To obtain the temperature field, these fringe images were processed by performing 2D fast Fourier transform, filtering the selected band of the spectrum, performing the inverse transform and phase unwrapping. The knowledge of the phase shift gives information about the gradient of refractive index, which is used to reconstruct 2D projections of the temperature field on the front and side view planes. The corresponding thermal fields (the first and last images in color in **Figure 7**) were restored from the interference patterns in **Figure 6**.

The transient development of vibrational mean flows was observed during a large number of microgravity periods with different levels of vibration (each period lasts around 20 s). Measurements of temperature field revealed large deviations from conductive state due to vibrational mean flows. The development of vibrational convection during experimental run with $Gs = 71.15 \times 10^3$ is shown in **Figure 7**.

The first picture from the left in **Figure 7** (0s) shows the temperature field in the cell (side view) at the beginning of the parabola when vibration is imposed. There are some deviations from a conductive state, which are small in the central region of the cell but become larger near the lateral walls due to heat fluxes through them. One of the reasons for temperature deviations is the weak convection caused by the residual gravity. The residual accelerations in the X and Y directions (perpendicular to the thermal gradient) can slightly destabilize vibrational mean flows. The analysis of different parabolas showed that the deviations from a conductive state were not large. Another reason can be associated with the fact that the walls are formed by two glass prisms, which can absorb heat. Note that thin regions (~0.2 mm) near the horizontal walls were inaccessible for optical measurements.

The development of thermovibrational flow causes the distortion of the temperature field, which is growing with time. The numerical snapshot taken at 1 s from the start of vibration reveals the mean flow structure with four vortices. The experimental thermal field also indicates the presence of this structure. The flow is not completely symmetrical because of the presence of residual gravity. This result is consistent with the predictions of two-dimensional numerical modeling [6]. The bifurcation from a symmetric pattern (1 s) to an asymmetric one (9 and 20 s) is observed. These images are recorded at different times but correspond to the same phase of vibration, in which the cell was in the focus of the camera.

Here, we would like to emphasize *the strategic* importance of the parabolic flights [25, 26] for the success of the IVIDIL experiment.

The IVIDIL experiment was carried out in the Selectable Optical Diagnostic Instrument, hosted in the Microgravity Science Glovebox (MSG) onboard the International Space Station. The SODI is a modular instrument with experiment-dependent exchangeable cells that are probed by means of optical interferometry (Mach-Zehnder). It is equipped with two Mach-Zehnder interferometers that can

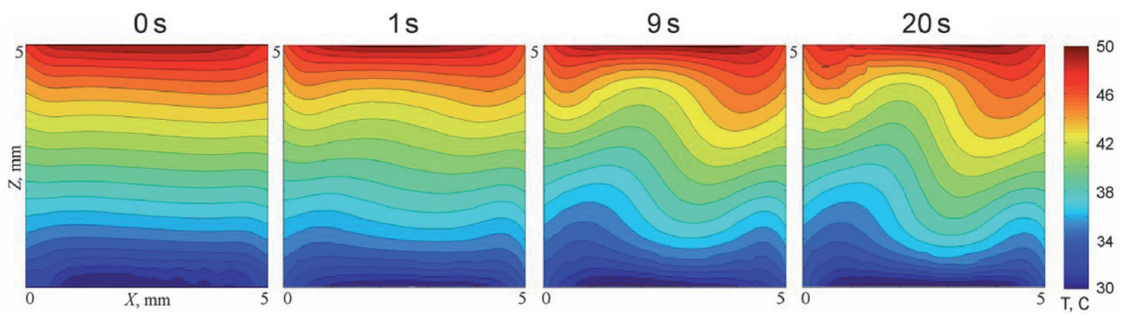

Figure 7.
The evolution of temperature field with time in the side view during the run with f = 4 Hz, A = 45 mm, ΔT = 20 K, Gs = 71,149.

Figure 8.
Science team moves from parabolic flights to the IVIDIL experiment.

be operated at two wavelengths (670 and 935 nm). The SODI allowed selecting a set of optical properties and the fringe spacing, depending on the performance requested by the scientists. In the case of IVIDIL, a total of two cell arrays consisting of two cells each have been analyzed.

This parabolic flight experiment in many aspects has a design similar to IVIDIL; in particular, the camera was mounted to the wall of a box at the end of the vibrational table. The camera had fixed frame rate (24 fps), and the cell vibrated at a given frequency. Thus, when the cell was moving, the camera recorded images both in and out of focus. We discussed with the ESA about a possible need to change the SODI design. However, the design of hardware was impossible to change, but the improvement was made by software on the image treatment. The camera records were synchronized with the frequency of the vibration in each experimental run.

Using all the experience obtained during the parabolic flight experiments, the team focused attention to the scientific part of the IVIDIL preparation [26] (see the team pictures in **Figure 8**).

6. Ground preparation and tests of the IVIDIL experiment

The full program of the IVIDIL experiment tests with participation of the science team consisted of several segments:

a. Numerical simulations

b. Cell filling at the QinetiQ Space company

c. Tests of the entire SODI facility imbedded inside the engineering model of Glovebox at the European Space Research and Technology Centre (ESTEC)

d. Familiarization tests at the Spanish User Support and Operations Centre (E-USOC, Madrid), which included testing the performance of the SODI facility onboard the ISS and its coordination with the on-site engineering model

6.1 Numerical simulations

Numerical programs in support of the IVIDIL experiment have been developed in two ways. The first one was devoted to the calculations of the 3D Navier-Stokes

equations using the geometry of the experiment and physical properties of liquid mixtures. For this, two international teams, one from Russia led by Prof. T. Lyubimova and the other from Canada led by Prof. Z. Saghir, have joined the MRC team. The numerical codes were benchmarked between the teams prior to the experiment to be conducted on ISS, and preliminary calculations were performed to select the best experimental parameters [9].

The second way was devoted to the development of codes for image processing and fitting of the experimental results to the analytical solution. Part of it was already done for parabolic flight experiments, but additional work was needed [1–3].

6.2 Cell filling

The cell filling with experimental liquids is a very delicate process. In the experiment with non-uniform temperature, concentration and vibrations, if any bubble would appear, the temperature and concentration fields in the cell would be strongly affected in several aspects. It would lead to Marangoni convection driven by the variation of surface tension on the bubble; in addition, a vibrating bubble would disturb the local flow field and mix the existing concentration gradient in an unwanted and uncontrolled way. Therefore, all experiment liquid solutions are degassed in vacuum chambers to remove all dissolved gases.

The science team prepared the solution mixtures in the MRC laboratories, degassed the solutions and delivered them to QinetiQ Space Company in sealed syringes as shown in **Figure 8**. The cell was filled in the QinetiQ Space by their experienced engineer in the presence of scientists and of an ESA representative. The procedure relies on evacuating the cell volume and then letting the sample be sucked from the syringe into the cell by the vacuum, as there is only one opening for filling. After the preliminary filling, the cell was inspected visually under 20 x magnification, to ascertain that no air is present in the sample. The image of the cell after the first run is shown on the left side in **Figure 9**. The bubbles found were removed manually by slightly tilting the cell array and forcing the bubbles through the filling hole.

The cell was inspected again and again, and after final inspection, the cell was sealed. The developed cell filling procedure brought an excellent result; the cells

Liquid delivered by the science team

The magnified view of the cell

Collaborative work of the science team, ESA and Qinetiq engineer.

Figure 9.
The IVIDIL flight cell filling on May 28, 2009.

were filled on May 28, 2009, and the IVIDIL experiment was completed 8 months later, and all the cells were bubble-free.

6.3 Tests of SODI-IVIDIL facility at the ESTEC

For any experiment on the ISS, at least two identical instruments are usually manufactured: the flight model and the engineering model. Most ground tests are performed using the engineering model. Delays in the manufacture of dedicated highly innovative instruments often occur, and it leads to a limited time for the ground testing. The SODI-IVIDIL facility placed inside the Glovebox model was tested in the ESTEC on February 23, 2009 and February 24, 2009.

The IVIDIL test procedure on the first day included four tests; in each of them, images were recorded during 180 s with sampling rate 10 s:

1. Isothermal cells $\Delta T = 0$, no vibration

2. Temperature gradient ΔT from above and below, no vibration

3. Temperature gradient ΔT from above and below, vibration of $f = 2$ Hz and $A = 25$ mm

4. Temperature gradient ΔT, vibration of highest forcing $f = 2.8$ Hz and $A = 31$ mm

(The tests were repeated two times: with and without personnel near the instrument)

The IVIDIL set-up consists of three principal parts (a cell array, a vibrational table and an optical system) as shown in **Figure 10**, right side. Cell array consists of two cells (as shown in **Figure 4c**) filled with the same binary mixture: the primary cell and the companion one, into which the particles are added. Each cell was monitored by the separate laser diode with wavelength $\lambda = 670$ nm.

After processing of recorded test images at the end of the day, it was found that the variation in contrast over images was quite high and not the same for different laser diodes. The next morning, we warned the developers of optical parts (Lambda-X) about the problems found, and in response, several parameters were changed. For example, the integration time of one of the cameras was increased, the

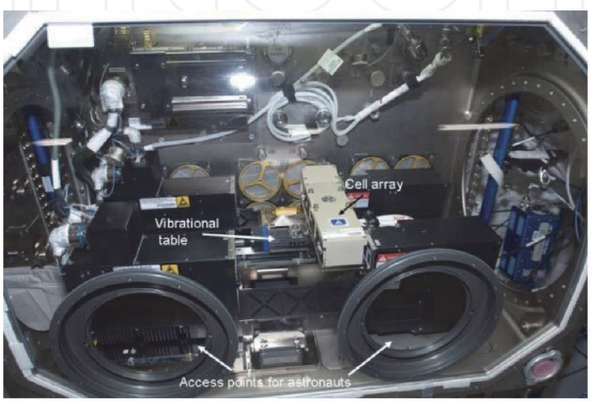

The IVIDIL set-up inside the Glovebox facility

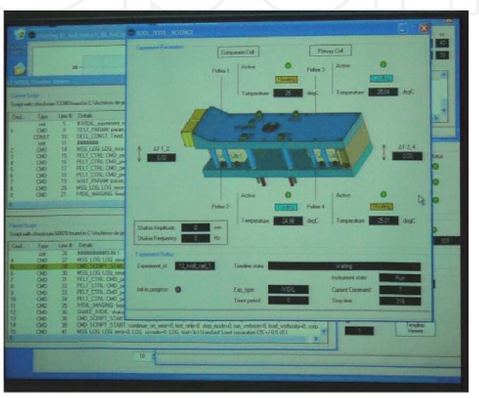

Real-time IVIDIL experiment screenshot at E-USOC

Figure 10.
SODI-IVIDIL on orbit and the experiment monitoring at the E-USOC.

laser temperature was changed, and the electrical current on laser was changed. All these small adjustments have led to a significant improvement in image quality.

The last part of the experiment preparation took place in the Spanish User Support and Operations Centre (E-USOC) in Madrid. To get a better understanding of the experiment hardware, and the possible in-flight changes of experimental parameters, the science team went to the E-USOC in Madrid in July 2009. During these days, the engineering model of SODI-IVIDIL was used to learn about in-flight operations and to simulate experimental runs. Also, telemetry software necessary for observation of the experiment during operations was installed and tested on the computers of the science team. The software for image processing was tested on data acquired with the engineering model. The E-USOC team working with SODI-IVIDIL was very dedicated and was very helpful in conducting all experiment preparations.

To conclude, all preparatory tests made essential contribution to the success of the experiment. However, the IVIDIL experiment overcomes the limits of ground tests which do not reproduce the space environment.

7. The IVIDIL on orbit

Shortly after arrival on orbit, on September 23, 2009, the SODI-IVIDIL was installed inside the Microgravity Science Glovebox in the Columbus laboratory by the ESA astronaut Frank De Winne and his Canadian crewmate Robert Thirsk. The activation of the IVIDIL experiment was scheduled on October 5, and the science teams as well as engineers from QinetiQ (Verhaert) Space were present at the E-USOC. The waiting time of the first image was exciting and nerve-wracking—does it really work? Are the images of good quality? The faces of the team at this breathtaking moment can be seen on the photos in **Figure 11**.

Yes, it worked!

Figure 11.
Waiting for the first response from IVIDIL in the E-USOC control room.

Since this memorable day, 55 experiments were conducted on the International Space Station. The experiment lasted from October 2009 to January 2010. Several interruptions occurred over this time, and they are related to the life onboard. First, it was surprising to learn that if there was a national holiday in one of the countries managing by the experiment, the experiment could run only in regime "unattended" or stopped, like it was during Christmas.

Second surprise was to find out that by default, astronauts do not work on Saturday and Sunday. Once, this nearly led to a critical situation. The first flash disk of the IVIDIL was nearly full and had to be replaced by another one. Among the astronauts onboard, only the ESA astronaut was trained to work with SODI-IVIDIL. His staying on the ISS was coming to an end, and the only chance to replace the disk was to do it on a Saturday. We asked through NASA if the ESA astronaut would accept to replace the disk as part of a volunteer work on a Saturday. He agreed and the disk was replaced.

Each experimental run lasted 18 h, and all the experiments were controlled via telescience provided by the European Spanish User Support and Operations Centre (E-USOC, Madrid), which means that the experiment science run was completely controlled from the ground without intervention of onboard astronauts. Part of the images acquired in each run was transmitted to the ground in real time, and a full set of images arrived on a flash disk a few months later, after completing the experiment. The science team stayed in the E-USOC for a week, until all the tests were completed and scientific runs started. Later, the control images and telemetry data were sent to Brussels on a daily basis on a specialized ftp server. At the very end, after completion of all the planned runs, we had the chance to ask several "nice to have" experiments which were interesting for science after quick analysis of the available results.

8. Scientific results of the IVIDIL

Preliminary results were obtained using a limited amount of data sent via telemetry. Thousands of recorded images returned to Earth on a flash disk a few months later. The experimental results have surpassed our expectations [27–32]. The experiment has been able to trace the variation of concentration of about 0.03% from the initial composition.

8.1 Impact of the onboard g-jitter on diffusion-controlled processes

After the numerous runs of the IVIDIL experiment, it was clearly demonstrated that only the major transient space station vibrations have an impact, such as those due to orbital debris avoidance maneuvers or dockings and undockings of a spacecraft. Furthermore, their impact depended on the duration of events. More common minor movements that are part of daily life aboard a space station did not affect the samples. Let us justify this statement.

The effect of the onboard environment on a diffusion-controlled process can be identified in the following ways: (a) by direct observation of temperature or concentration fields and their smoothness; (b) by comparing fields along two perpendicular views; (c) by reproducibility of experimental results when repeating experiment on different days and thus in a different microgravity environment; (d) by comparing with computations in the absence of perturbations; and (e) by observation of g-jitter-induced convection, in the case that it arises.

In the steady state, when mixture has Soret effect, the concentration field and the temperate field have similar distributions (here ST is the Soret coefficient):

$$C - C0 = -ST\,(T - T0). \tag{5}$$

The steady-state distribution of the temperature field measured onboard is shown in one of the views in **Figure 12**, left side. The temperature field is set within a few minutes, while the concentration field takes more than 10 hours to reach the steady state. Thus, the concentration field is more susceptible to the influence of g-jitter.

The concentration (temperature) field was recorded in two perpendicular directions, as shown in **Figure 4**. Accordingly, in the experiments, when the imposed vibrations are absent or weak, the images should be similar in both directions if they are not perturbed by the microgravity environment. **Figure 12** (right side) provides an appropriate illustration of the absence of perturbations. The central part of the figure presents five isosurfaces of equal concentrations of the experiment at the end of the thermodiffusion step, after 12 h of Soret separation. The midsurface (green) corresponds to the initial concentration $C_0 = 0.90$, and the following surfaces are separated by $\delta C = 6 \times 10^{-4}$.

This 3D concentration field reveals no significant disturbances due to onboard accelerations, except for small ripples of isolines typical of most experiments. The distributions on the sides show averaged concentration fields in perpendicular directions, which are almost identical. Note that these concentration distributions on the sides are similar to the temperature field on the left side of the **Figure 12**.

Several experiments without imposed vibrations were conducted on different days (even months) and for two different binary mixtures. On one of the days, the gravitational environment had stronger perturbations, measured by the Space Acceleration Measurement System (SAMS) instrument. It resulted in a slightly larger scattering of the experimental points [27], but the final results coincided with those from the other days and with the numerical separation for the free-convection case.

Another experiment, with imposing weak vibrational forcing, $gos/g0 = 7.0 \times 10^{-4}$, was repeated with an interval of 2 weeks. The measured value of the Soret separation, ΔC, which is the concentration difference at the hot and cold walls, was almost identical. Furthermore, the ΔC value for these experiments was similar to

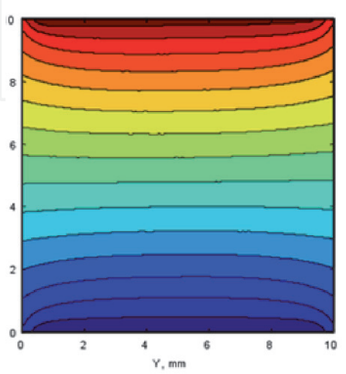

Temperature field at t=10min after imposing ΔT=5K

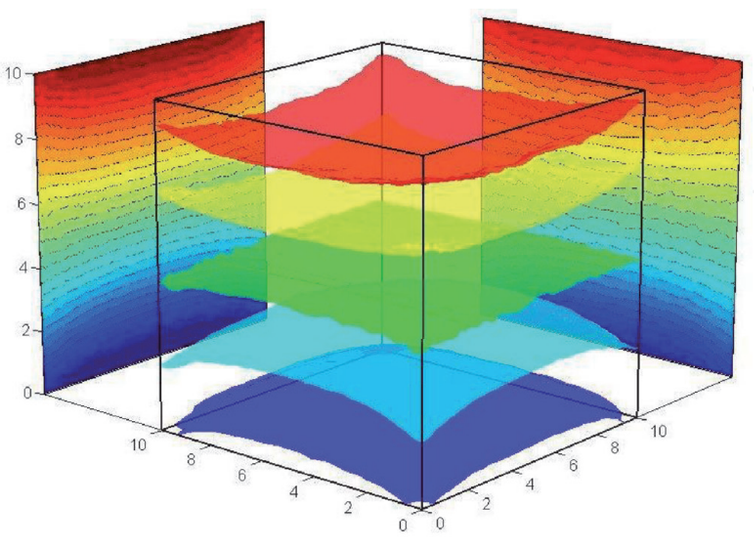

Measured concentration field after 12 h of Soret separation. Five isosurfaces of equal concentrations are shown at the centre. The distributions on the sides show averaged concentration fields in perpendicular directions.

Figure 12.
Measured temperature and concentration field in g-jitter environment of the ISS.

that one obtained in the experiments carried out only in g-jitter environment. These observations emphasize that neither the weak imposed vibrations nor onboard accelerations affect the process of diffusion.

Note that these results may not be applicable in the case of the large peak accelerations that occur on the ISS due to the maintenance of the station or in case of a fluid system with a sharp difference in density (e.g. gas/liquid interface).

8.2 Development of mean flow under the action of periodic forcing

The IVIDIL experiment also demonstrated that, unlike g-jitter, imposed vibrations with constant frequency and amplitude do affect the diffusion process. High-frequency periodic forcing with a zero mean value causes time-averaged (mean or streaming) flows, which substantially affect the regime of mass transfer in a fluid.

The physical mechanisms through which mean flows modify thermal and concentration fields in a binary mixture with a negative Soret effect (water-isopropanol 90–10%) were examined. The evolution of the mean flows is the result of a nonlinear interaction between thermal, solutal and vibrational effects. Because vibrations act on a mixture with non-uniformities in density, the development of the mean flows depends on this gradient. The vibrations were activated 10 min after imposing a temperature gradient ΔT. By that time, the initial density stratification was created by the thermal field in the cell and the concentration gradients very near the solid walls. First, on a short time scale, the vibrations create significant mean flows due to the presence of density gradients primarily induced by thermal non-uniformities. Then, concentration variations caused by a slow Soret effect change the density gradients that drive vibrational convection, which in turn modifies the concentration field. The density gradient caused by a negative Soret effect is opposite to that created by the thermal field and reduces the net density gradient. Thus, the growth of perturbations in a concentration field is decelerated.

Two regimes of mass transfer were identified, depending on vibrational forcing: diffusive for $Gs < 1200$ and convective for $Gs > 1200$. In the diffusive regime, the Soret separation decreases linearly with an increase in Gs, and the mean flow begins to affect the distribution of the concentration field. The example of the concentration field and its cross-section in two perpendicular directions at the central part is shown in **Figure 13** when $Cs = 910$. One may compare this concentration field with that one in **Figure 12**, obtained in g-jitter environment. In the g-jitter environment, the isosurfaces were almost flat, just slightly bended toward the wall due to temperature nonlinearity on the walls. The concentration field in **Figure 13** is deformed by the mean flow which has four-roll structure.

To simplify the understanding, the computed flow pattern is shown on the right side of the figure. This flow pattern is shown via trajectories of liquid particles. The small-amplitude oscillations (fast) correspond to the imposed frequency, and the four large rolls illustrate convective motion (mean flow). The velocity of "fluid particles" that exhibit fast oscillatory motion while moving around the vortex is 100 times higher than the velocity of the mean flow (1–10 mm/s) and is of the same order of magnitude as the characteristic viscous velocity L/ν.

In the convective regime, $Gs > 1200$, the mean flow is strong enough to trap the concentration near the walls and maintains a constant flow velocity in the bulk. Close to the $Cs = 1200$, the flow pattern keeps the same four-roll structure which progressively deforms with further increase of vibrational forcing.

In the frame of a postflight study, the vibrational environment (g-jitter) recorded by the SAMS instrument during the IVIDIL experiment was analyzed [33–35] as well as its possible influence of the Soret separation [36]. The study shows that during experimental runs, there were no major perturbations of the microgravity

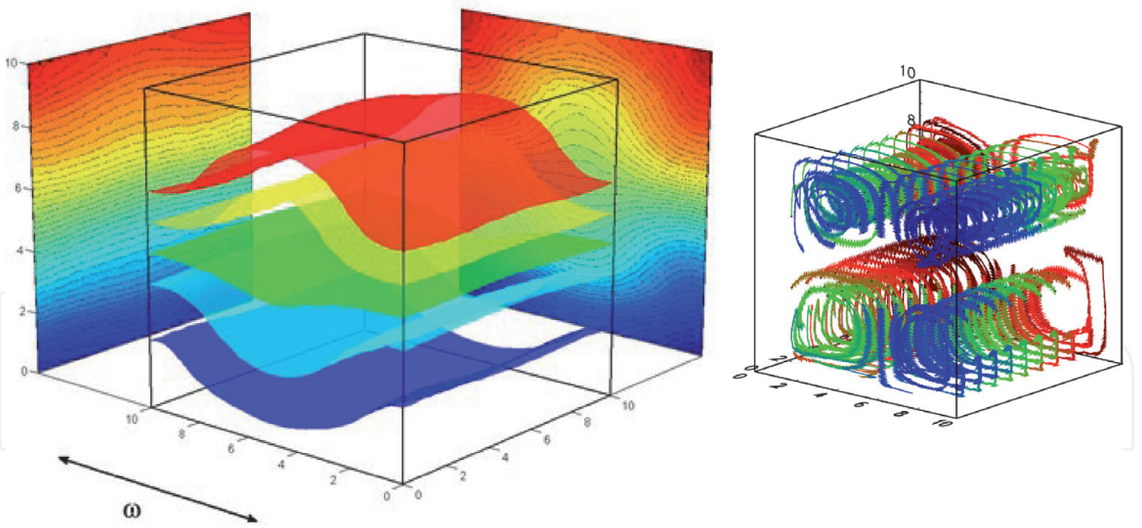

The 3D (tomographic reconstruction) concentration field and its cross-section in two perpendicular directions at the central part in case of imposed vibration

The fluid particles are moving along the mean flow streamlines while performing fast oscillatory motion with small amplitude

Figure 13.
(Left) The concentration field in diffusive regime restored from the IVIDIL data, Gs = 910. (Right) Numerical presentation of the flow pattern for this regime.

environment. However, an unknown frequency equivalent to the third harmonic, but with large amplitude, was recorded during runs at which the strongest vibrational forcing was applied. A more detailed study suggests that, with high vibrational excitations, the linear motor also generates lateral cell motion perpendicular to the main direction. The interactions of these movements lead to the generation of additional frequencies acting on the liquid mixture.

9. Conclusions

In order to take full advantage of the unique opportunity of ISS experiments, the ground-based preparations are indispensable.

Ground experiments are aimed at confirming the operating principle of onboard equipment and motivate the development of codes that will be used to process the microgravity results.

The creation and use of mathematical models is another key element of preparation. Mathematical modeling provides the characteristic scales and the range of parameters that may be beneficial for research. However, any mathematical model contains many assumptions and idealizations. A comparison of numerical predictions and ground-based observations, although perturbed by gravity, can rearrange the set of parameters used in microgravity.

The culmination of ground-based preparation is the tests on parabolic flights. A lot of useful data can be collected from parabolic flight experiments, and they may even call for modification of the onboard installation before heading further into space.

IntechOpen

Author details

Valentina Shevtsova*, Denis Melnikov, Yuri Gaponenko and Aliaksandr Mialdun
Microgravity Research Centre, Université libre de Bruxelles (ULB), Brussels, Belgium

*Address all correspondence to: vshev@ulb.ac.be

References

[1] Mialdun A, Shevtsova V. Development of optical digital interferometry technique for measurement of thermodiffusion coefficients. International Journal of Heat and Mass Transfer. 2008;**51**: 3164-3178

[2] Mialdun A, Shevtsova V. Digital interferometry as a powerful tool to study the thermodiffusion effect. Comptes Rendus Mecanique. 2011;**339**: 362-368

[3] Mialdun A, Shevtsova V. Measurement of the Soret and diffusion coefficients for benchmark binary mixtures by means of digital interferometry. The Journal of Chemical Physics. 2011;**134**:044524

[4] Mialdun A, Shevtsova V. Measurement of Soret coefficients: Open questions. Microgravity Science and Technology. 2009;**21**:31-36

[5] Mialdun A, Ryzhkov I, Melnikov D, Shevtsova V. Experimental evidence of thermovibrational convection in low gravity. Physical Review Letters. 2008; **101**:084501

[6] Shevtsova V, Ryzhkov I, Melnikov D, Gaponenko Y, Mialdun A. Experimental and theoretical study of vibration-induced thermal convection in low gravity. Journal of Fluid Mechanics. 2010;**648**:53-82

[7] Shevtsova V, Gaponenko Y, Melnikov D, Ryzhkov I, Mialdun A. Study of thermoconvective flows induced by vibrations in reduced gravity. Acta Astronautica. 2010;**66**:166-173

[8] Melnikov D, Ryzhkov I, Mialdun A, Shevtsova V. Thermovibrational convection in microgravity: Preparation of a parabolic flight experiment. Microgravity Science and Technology. 2008;**20**(1):29-39

[9] Shevtsova V, Melnikov D, Legros JC, Yan Y, Saghir Z, Lyubimova T, et al. Influence of vibrations on thermodiffusion in binary mixture. Benchmark of numerical solutions. Physics of Fluids. 2007;**19**:017111

[10] Melnikov D, Shevtsova V, Legros JC. Impact of conditions at start-up on thermovibrational convective flow. Physical Review E. 2008;**78**(5): 056306

[11] Gershuni GZ, Lyubimov DV. Thermal Vibrational Convection. New York: Wiley & Sons; 1998

[12] Gaponenko YA, Torregrosa M, Yasnou V, Mialdun A, Shevtsova V. Dynamics of the interface between miscible liquids subjected to horizontal vibration. Journal of Fluid Mechanics. 2015;**784**:342-372

[13] Beysens D. Vibrations in space as an artificial gravity? Europhysics News. 2006;**37**:22

[14] Wolf GH. Dynamic stabilization of the interchange instability of a liquid–gas interface. Physical Review Letters. 1970;**24**:444-446

[15] Gaponenko Y, Torregrosa M, Yasnou V, Mialdun A, Shevtsova V. Interfacial pattern selection in miscible liquids under vibration. Soft Matter. 2015;**11**:8221-8224

[16] Savino R, Monti R. Physics of Fluids in Microgravity. London: Taylor & Francis; 2001. p. 178

[17] Hirata K, Sasaki T, Tanigawa H. Vibrational effects on convection in a square cavity at zero gravity. Journal of Fluid Mechanics. 2013;**445**:327-344

[18] Demin VA, Gershuni GZ, Verkholantsev IV. Mechanical quasi-

equilibrium and thermovibrational convective instability in an inclined fluid layer. International Journal of Heat and Mass Transfer. 1996;**39**:1979

[19] Gershuni GZ, Kolesnikov AK, Legros JC, Myznikova BI. On the vibrational convective instability of a horizontal, binary-mixture layer with Soret effect. Journal of Fluid Mechanics. 1997;**330**:251

[20] Zebib A. Low-gravity sideways double-diffusive instabilities. Physics of Fluids. 2001;**13**:1829-1832

[21] Lyubimova TP, Shklyaeva E, Legros JC, Shevtsova V, Roux B. Numerical study of high frequency vibration influence on measurement of Soret and diffusion coefficients in low gravity conditions. Advances in Space Research. 2005;**36**:70-74

[22] Zyuzgin AV, Ivanov AI, Polezhaev VI, Putin GF, Soboleva EB. Convective motions in near-critical fluids under real zero-gravity conditions. Cosmic Research. 2001; **39**(2):175

[23] Garrabos Y, Beysens D, Lecoutre C, Dejoan A, Polezhaev V, Emelianov V. Thermoconvectional phenomena induced by vibrations in supercritical SF6 under weightlessness. Physical Review E. 2007;**75**:056317

[24] Babushkin IA, Bogatyrev GP, Glukhov AF, Putin AF, Avdeev SV, Ivanov I, et al. Investigation of thermal convection and low-frequency microgravity by the DACON sensor aboard the MIR orbital complex. Cosmic Research. 2001;**39**(2):161-169

[25] TEVICON. Transient time of thermal-vibrational convection in reduced gravity, Erasmus Experiment Archive, Experiment Record N° 8990. Available from: http://eea.spaceflight.esa.int/portal/exp/?id=8990 [Last consulted: 19 February 2020]

[26] TEVICON-1. Thermo-vibrational convection in reduced gravity, Erasmus Experiment Archive, Experiment Record N° 9027. Available from: http://eea.spaceflight.esa.int/portal/exp/?id=9027 [Last consulted: 19 February 2020]

[27] Shevtsova V. IVIDIL experiment onboard the ISS. Advances in Space Research. 2010;**46**(5):672-679

[28] Shevtsova V, Lyubimova T, Saghir Z, Melnikov D, Gaponenko Y, Sechenyh V, et al. IVIDIL: On-board g-jitters and diffusion controlled phenomena. Journal of Physics: Conference Series. 2011;**327**:012031

[29] Mazzoni S, Shevtsova V, Mialdun A, Melnikov D, Gaponenko Y, Lyubimova T, et al. Vibrating liquids in space. Europhysics News. 2010;**41**:14

[30] Shevtsova V, Gaponenko YA, Sechenyh V, Melnikov DE, Lyubimova T, Mialdun A. Dynamics of a binary mixture subjected to a temperature gradient and oscillatory forcing. Journal of Fluid Mechanics. 2015;**767**:290-322

[31] Shevtsova V, Mialdun A, Melnikov D, Ryzhkov I, Gaponenko Y, Saghir Z, et al. IVIDIL experiment onboard ISS: Thermodiffusion in presence of controlled vibrations. Comptes Rendus Mecanique. 2011;**339**:310-317

[32] Mialdun A, Yasnou V, Shevtsova V, Koeniger A, Koehler W, Alonso de Mezquia D, et al. A comprehensive study of diffusion, thermodiffusion, and Soret coefficients of water-isopropanol mixtures. The Journal of Chemical Physics. 2012;**136**(24):244512-244513

[33] Sáez N, Ruiz X, Gavaldà F, Shevtsova V. Comparative analyses of ESA, NASA and JAXA signals of acceleration during the SODI-IVIDIL experiment. Microgravity Science and Technology. 2014;**26**:57-64

[34] Sáez N, Ruiz X, Jna.Gavaldà, Pallarés J, Shevtsova V. Comparative ISS accelerometric analyses. Acta Astronautica. 2014;**94**:681-689

[35] Sáez N, Jna.Gavaldà, Ruiz X, Shevtsova V. Detecting accelerometric nonlinearities in the international space station. Acta Astronautica. 2014;**103**: 16-25

[36] Gaponenko Y, Mialdun A, Shevtsova V. Experimental and numerical analysis of mass transfer in a binary mixture with Soret effect in the presence of weak convection. European Physical Journal. 2014;**37**:90